Available online at www.sciencedirect.com
ScienceDirect
International Journal of Heat and Mass Transfer 50 (2007) 5041–5053
International Journal of HEAT and MASS TRANSFER
www.elsevier.com/locate/ijhmt

Modeling of the condensation sink term in an interfacial area transport equation

Hyun-Sik Park [a,*], Tae-Ho Lee [b,1], Takashi Hibiki [c], Won-Pil Baek [a], Mamoru Ishii [c,2]

[a] Thermal Hydraulics Safety Research Center, Korea Atomic Energy Research Institute, 1045 Daedeokdaero, Yuseong, Daejeon 305-353, Republic of Korea
[b] Fast Reactor Development Group, Korea Atomic Energy Research Institute, 1045 Daedeokdaero, Yuseong, Daejeon 305-353, Republic of Korea
[c] School of Nuclear Engineering, Purdue University, 400 Central Drive, West Lafayette, IN 47907, USA

Received 10 January 2007; received in revised form 17 August 2007
Available online 23 October 2007

Abstract

A model for the condensation sink term in an interfacial area transport equation (IATE) was developed. In the model, a bubble nucleation due to a wall surface boiling and a bubble collapse due to a condensation were assumed to be symmetric phenomena. Based on this consideration the condensing region for a subcooled condition can be divided into two regions: the heat transfer-controlled region and the inertia-controlled region. In the heat transfer-controlled region, the condensation Nusselt number approach is appropriate. On the other hand, in the inertia-controlled region, the resultant mechanical force may be balanced through an interface between a bubble and an ambient liquid. The modeled condensation sink term in an IATE in this study was evaluated against existing data which had been obtained from a bubble condensation in a subcooled water flow through a non-heated annulus. The evaluation result showed that the present model could predict the axial distribution of the interfacial area concentration accurately.

Keywords: Interfacial area transport equation; Condensation; Bubble collapse; Sink term modeling

1. Introduction

The existence of interfacial transfer terms is one of the most important characteristics of a two-fluid model formulation. Generally, these interfacial transfer terms are expressed as the product of an interfacial area concentration (IAC) and a driving force. Thus an accurate prediction of an IAC is one of the most important factors in a two-fluid model. Recently an interfacial area transport equation (IATE) was introduced to predict an IAC mechanistically [1]. The general form of an interfacial area transport equation [2] has various source and sink terms which include a bubble breakup, a bubble coalescence, an expansion or shrinkage due to a phase change and a pressure change, a bubble condensation, and a wall nucleation.

For a general application of an IATE to a two-phase flow, reliable constitutive relations for the relevant source and sink terms should be developed. For an adiabatic two-phase flow, some models for these source and sink terms have been developed based on the mechanisms of a coalescence and a disintegration of fluid particles by several researchers for various experimental conditions and test geometries [3–7]. Significant efforts have been made for a one-group IATE, which is applicable to a bubbly flow, by using various modeling approaches [3,4], and recently a one-group IATE was evaluated by the data taken from an adiabatic air–water bubbly flow in a vertical annulus [5]. Furthermore, in order to capture the effect of a bubble size on a flows' nature, a general approach to treat the bubbles of two groups, namely spherical and distorted bubbles as a group-I bubble, and cap, slug and

* Corresponding author. Tel.: +82 42 868 8615; fax: +82 42 861 6438.
E-mail addresses: hspark@kaeri.re.kr (H.-S. Park), thlee@kaeri.re.kr (T.-H. Lee), hibiki@ecn.purdue.edu (T. Hibiki), wpbaek@kaeri.re.kr (W.-P. Baek), ishii@ecn.purdue.edu (M. Ishii).
[1] Tel.: +82 42 868 8975.
[2] Tel.: +1 765 496 9033; fax: +1 765 494 9570.

0017-9310/$ - see front matter © 2007 Elsevier Ltd. All rights reserved.
doi:10.1016/j.ijheatmasstransfer.2007.09.001

Nomenclature

A_c	cross-sectional area of the flow channel [m^2]
A_b	interfacial area of a bubble [m^2]
a_i	interfacial area concentration [1/m]
D	bubble diameter [m]
D_b	bubble diameter at the region boundary [m]
D_c	critical collapsing bubble diameter [m]
D_d	bubble diameter generated during nucleation [m]
D_{sm}	Sauter mean bubble diameter [m]
f	bubble generation frequency from active nucleation sites [1/s]
h_c	condensation heat transfer coefficient [W/(m^2 s)]
h_{fg}	latent heat of vaporization [J/kg]
k	thermal conductivity [W/(m K)]
$\dot{m}_c$	condensation mass flow rate [kg/s]
N_{cn}	active nucleation site density [#/m^2]
Nu_c	condensation Nusselt number [–]
P	pressure [Pa]
p_c	fraction of bubbles in the inertia-controlled region [–]
R	gas constant [J/(mol K)]
R_{ph}	the change rate of the bubble number due to phase change [#/(m^3 s)]
T	temperature [°C]
t	time [s]
t_c	bubble collapsing time [s]
v_b	volume of a bubble [m^3]

Greek symbols

α	void fraction [–]
α_t	thermal diffusivity [m^2/s]
β	non-dimensional bubble diameter ($=D/D_0$) [–]
β_b	non-dimensional bubble diameter at the boundary ($=D_b/D_{sm}$) [–]
Γ_g	mass transfer rate per unit mixture volume [kg/(m^3 s)]
ξ_h	heated perimeter of the boiling channel [m]
η_{ph}	volume change rate per unit mixture volume [1/s]
σ	surface tension [N/m]
ϕ	the change rate of bubble number per unit mixture volume [#/(m^3 s)] or the change rate of the interfacial area concentration [1/(m s)]

Subscripts

a	area averaged
b	bubble
BB	bubble breakup
BC	bubble coalescence
CD	total condensation
CO	condensation in the inertia-controlled region
f	liquid
i	interface
in	inertia-controlled region
g	gas
PC	condensation in the heat transfer-controlled region
ph	phase change
PV	volume change due to the pressure change
RC	random collision
sub	subcooled
sat	saturation
TI	turbulence impact
th	heat transfer-controlled region
v	vapor
WN	wall nucleation
0	practical incipience boiling point

churn turbulent bubbles as a group-II bubble, has been proposed [2]. The basic concept of a two-group IATE was demonstrated for the interactions between two groups of bubbles at the transition from a bubbly to a slug flow [6] and it was also solved for a confined gas–liquid two-phase flow, which is applicable to bubbly, cap-turbulent, and churn-turbulent flow regimes [7]. The two-group IATE is reduced to a one-group IATE in a bubbly flow regime where no group-II bubbles exist. More recently, one-group and two-group IATEs available for an adiabatic two-phase flow were reviewed including the evaluation results obtained through extensive experimental studies [8].

However, for a boiling or condensing flow, the appropriate source and sink models to account for a phase change have not been developed as yet. The source term due to a wall nucleation can be expressed by the relation between an active nucleation site density, a bubble lift-off diameter, and a bubble lift-off frequency [9]. However, reliable models for a bubble lift-off diameter and a bubble lift-off frequency have not been properly proposed until now. Recently, an active nucleation site density has been modeled mechanistically [10] and forced convective subcooled boiling flow experiments have been conducted in a BWR-scaled vertical upward annular channel to formulate the dimensionless form of a bubble lift-off diameter [11]. The modeling work for a condensation sink term has also been limited thus far. In boiling and condensing flows, the condensation sink and nucleation source terms are expected to be dominant. Thus extensive efforts to model these two terms are required to develop a general IATE in the future.

As a part of developing a reliable IATE which can be applicable to a two-phase bubbly flow accompanied with a phase change, a model for the condensation sink term in an IATE is proposed in this study. For a collapsing

bubble, two kinds of collapsing mechanisms are possible. One is due to the resultant liquid inertia and the other is due to a heat transfer through the interface [12]. In the model, the condensation of a bubble is considered to occur in two subsequent regions: the heat transfer-controlled region and the inertia-controlled region. Based on the bubble collapse phenomena, these two regions are identified by introducing the concept of a boundary bubble diameter and then the bubble collapse time in a heat transfer-controlled region is calculated. The probability of bubbles in the inertia-controlled region is also calculated based on a residence time. Finally, a condensation sink term model is derived based on a steady one-dimensional form of an IATE and the developed model is evaluated against existing IAC data [13] which was obtained from a steam-water condensing flow where no wall nucleation occurred.

2. Interfacial area transport equation

Kocamustafaogullari and Ishii [9] formulated a bubble number density transport equation in terms of a differential balance equation which takes into account various effects such as a bulk liquid nucleation, a wall cavity nucleation and the bubble collapse rates. Considering a boiling channel with a constant cross-sectional area and by neglecting a bulk liquid bubble nucleation and a disintegration and coalescence of the bubbles, a one-dimensional transport equation for predicting the average bubble number density can be expressed as

$$\frac{\partial N_b}{\partial t}+\frac{\partial}{\partial z}(N_b v_{bz})=\phi_{WN}-\phi_{CD} \tag{1}$$

where N_b, t, v_{bz}, ϕ_{WN}, and ϕ_{CD} are the bubble number density, the time, the average bubble velocity, the bubble nucleation rate from the active sites and the bubble sink rate due to a condensation, respectively. The source term due to a bubble nucleation on a heated surface wall is expressed as

$$\phi_{WN}=(N_{cn} f \xi_h)/A_c \tag{2}$$

where N_{cn}, f, ξ_h, and A_c are the active nucleation site density, and the bubble generation frequency from the active sites, and the heated perimeter and the cross-sectional area of the boiling channel, respectively.

They showed that the bubble number sink rate is due to either a coalescence of small bubbles into a larger bubble or a re-condensation of the bubbles in a subcooled bulk fluid. The coalescence was assumed to be insignificant up to a void fraction of 0.3, beyond which a flow regime transition to a slug or churn-turbulent flow occurs. The highly subcooled boiling region of a flow channel is of little significance as far as the net bubble generation rate is concerned and its transition point is regarded as the point of a net bubble generation. They assumed that the bubble number sink rate could be calculated based on the re-condensation rate of the generated bubbles. The fraction of a re-condensation in the region downstream of a transition point can be obtained by comparing the rates of a net vapor generation and an evaporation at a wall's surface. The sink term due to a condensation in a subcooled liquid is expressed as [9]

$$\phi_{CD}=(T_{sat}-T_f)/(T_{sat}-T_0)\cdot\phi_{WN} \tag{3}$$

where T_{sat}, T_f, and T_0 are the saturation temperature, the bulk liquid temperature, and the bulk liquid temperature at the practical boiling incipience point, respectively. However, this modeling approach is not applicable to a bubble condensation in a subcooled liquid without any heat addition from a wall.

Ishii et al. [1,2] also derived an interfacial area transport equation from a statistical model of a fluid particle number transport equation. The general form of their interfacial area transport equation is given by the following equation:

$$\begin{aligned}\frac{\partial a_i}{\partial t}+\nabla(a_i v_i)&=\frac{2}{3}\left(\frac{a_i}{\alpha}\right)\left(\frac{\partial\alpha}{\partial t}+\nabla(\alpha u_g)-\eta_{ph}\right)\\&\quad+\frac{1}{3\psi}\left(\frac{\alpha}{a_i}\right)^2\sum_j R_j+\pi D_{ph}^2 R_{ph}\\&\approx\frac{2}{3}\left(\frac{a_i}{\alpha}\right)\left(\frac{\partial\alpha}{\partial t}+\nabla(\alpha u_g)\right)\\&\quad+\frac{1}{3\psi}\left(\frac{\alpha}{a_i}\right)^2\sum_j R_j+\pi D_{ph}^2 R_{ph}\\&=\frac{2}{3}\left(\frac{a_i}{\alpha}\right)\left(\frac{\Gamma_g}{\rho_g}-\frac{\alpha}{\rho_g}\left(\frac{\partial\rho_g}{\partial t}+u_g\cdot\nabla\rho_g\right)\right)\\&\quad+\frac{1}{3\psi}\left(\frac{\alpha}{a_i}\right)^2\sum_j R_j+\pi D_{ph}^2 R_{ph}\end{aligned} \tag{4}$$

where a_i, v_i, α, u_g, η_{ph}, ψ, D_{ph}, R_j, R_{ph}, and Γ_g are the interfacial area concentration, the interfacial velocity, the void fraction, the bubble velocity, the rate of volume generated by a phase change per unit mixture volume, a factor depending on the shape of the bubbles, the critical bubble size, the changing rate of an IAC due to a bubble breakup or coalescence, the changing rate of an IAC due to a phase change, and the rate of an interfacial phase change per unit mixture volume, respectively. The total change of an interfacial area concentration is expressed in terms of the changes due to the pressure, the particles interactions and a phase change. The term η_{ph} is negligibly small when compared with the other terms.

For a relatively uniform void distribution with no heat addition from a wall, a one-dimensional interfacial area transport equation can be obtained by integrating Eq. (4) over the flow channel as follows:

$$\frac{\partial\langle a_i\rangle}{\partial t}+\frac{\partial}{\partial z}\langle a_i\rangle\langle\langle v_{iz}\rangle\rangle_a = \frac{2}{3}\left(\frac{\langle a_i\rangle}{\langle\alpha\rangle}\right)\left(\frac{\langle\Gamma_g\rangle}{\rho_g}-\frac{\langle\alpha\rangle}{\rho_g}\left(\frac{\partial\rho_g}{\partial t}+\langle\langle v_{gz}\rangle\rangle\frac{\partial}{\partial z}\langle\rho_g\rangle\right)\right) + \frac{1}{3\psi}\left(\frac{\langle\alpha\rangle}{\langle a_i\rangle}\right)^2\sum_j\langle R_j\rangle+\pi\langle D_{ph}\rangle^2\langle R_{ph}\rangle = \phi_{PC}+\phi_{PV}+\phi_{BB}+\phi_{BC}+\phi_{CO} \quad (5)$$

Each term of the above IATE is explained as follows. ϕ_{PC} and ϕ_{PV} mean the source and sink terms of an expansion or shrinkage due to a phase change and a pressure change, respectively. ϕ_{BB} and ϕ_{BC} mean the source term due to a bubble breakup and the sink term due to a bubble coalescence, respectively, and ϕ_{CO} means the sink term due to a bubble condensation. When the wall nucleation term is considered, the void fraction may be localized near a wall. In this case a bubble-layer thickness model [14] can be utilized to avoid covariance terms.

Eq. (5) can be further simplified under steady state conditions for a condensing flow without a wall nucleation as follows:

$$\frac{\partial}{\partial z}(\langle a_i\rangle\langle v_{iz}\rangle_a)=\phi_{PC}+\phi_{PV}+\phi_{BB}+\phi_{BC}+\phi_{CO} \quad (6)$$

The source and sink terms of ϕ_{BB} and ϕ_{BC} have been modeled successfully, particularly in a bubbly flow regime, and they can be estimated easily by an existing model [4]. The source and sink terms of ϕ_{PV} are given by an explicit function of the void fraction, the bubble velocity and the pressure gradient [2–4,15]. The modeling approach for the condensation sink terms of ϕ_{PC} and ϕ_{CO} is described in the next section.

3. Mechanism of a bubble collapse

3.1. Simplified mechanism of a bubble collapse

A bubble generation due to a boiling and a bubble extinction due to a condensation are symmetrical phenomena. Fig. 1 shows a typical variation of the bubble size during a boiling and condensation process [16,17]. A bubble is generated abruptly from the heated surface ($A \rightarrow B$) and the initial bubble growth is very rapid ($B \rightarrow C$), but as the size increases the growth rate slows down ($C \rightarrow D$). When the bubble attains a maximum diameter (D) and departs from the superheated region, it starts collapsing in the ambient subcooled liquid ($D \rightarrow E$). At a low subcooling the bubble collapse is mainly controlled by a heat transfer. However, with a decrease of the bubble size ($E \rightarrow F$) and an increase of the liquid subcooling the bubble can not sustain its interfacial boundary anymore and it is collapsed by inertia during a short time period ($F \rightarrow G$). From the previous studies on the behavior of a bubble motion in a subcooled liquid, it is assumed that there are four regions during the lifetime of a bubble. Region I is the bubble generation region in an ambient superheated condition, Region II the bubble growth region in a superheated condition, Region III the bubble shrink region in a subcooled condition, and Region IV the bubble collapse region in a subcooled condition. Regions I and IV have very short periods of a residence time. In Fig. 1, D_d is the bubble diameter at point B which is attained through an inertia-controlled bubble growth process during a nucleate boiling, D_b is the bubble diameter at point F when the bubble becomes controlled by the inertia during a bubble condensation, and D_c is the critical collapsing bubble diameter at point G. As shown in Fig. 1, the condensing region in the subcooled condition can be divided into two regions: the heat transfer-controlled region (Region III) and the inertia-controlled region (Region IV). In the heat transfer-controlled region, the Nusselt number approach is appropriate. However, in the inertia-controlled region the bubbles are collapsed by the inertia of the surrounding liquid during a short time period.

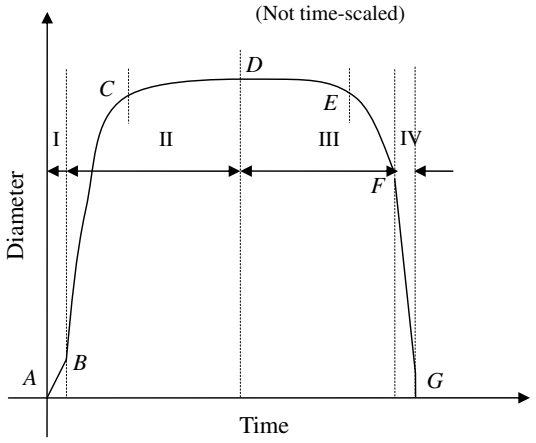

Fig. 1. Variation of the bubble size during the boiling and condensation process.

When a vapor bubble in a saturated condition is surrounded by an ambient subcooled liquid, a condensation occurs through an interface. In the beginning, the condensation phenomena are controlled by a heat transfer through this interface. As the condensation process continues through the interface between the vapor bubble and the ambient liquid, the bubble diameter decreases and so does the vapor temperature inside the bubble. When the bubble size reaches a boundary bubble size (F), the size does not decrease gradually by a heat transfer through the interface but it collapses very rapidly due to mechanical inertia. An arbitrary cut-off diameter of the bubble can be used to identify the sudden collapse of a bubble from a gradual decrease of the bubble size. At the end of the inertia-controlled region, the critical collapsing bubble size can be calculated in terms of the liquid temperature from the resultant mechanical force balance. After the bubble size decreases to the critical collapsing bubble diameter (G), it disappears. A certain amount of a pressure difference

between the bubble and the ambient liquid is necessary to maintain a bubble shape during the condensation process. If the pressure difference is considerably small, the bubble can not survive any longer and it disappears. The critical collapsing bubble size can be calculated from the pressure balance between the vapor bubble and the ambient liquid, which is described in Appendix A.

3.2. Region identification and boundary bubble diameter

When the bubble size decreases gradually, it is in the heat transfer-controlled region. If the changing rate of a bubble diameter increases rapidly, the bubble is in the inertia-controlled region. The criteria of a transition can be determined from previous theoretical and experimental observations [18–20]. A spherical shape is unstable for a rapidly collapsing bubble near the end of its collapse [18]. From the analysis of a collapsing vapor bubble in liquids [19,20] the decreasing rate of the bubble size is very rapid at the end of its lifetime. It is assumed that the bubble is in the inertia-controlled region after the bubble size starts to decrease very rapidly.

There are two possible criteria to separate the inertia-controlled region from the heat transfer-controlled region. One is the decreasing rate of a bubble size and the other is the size of a bubble itself. As the change of a bubble size is not easy to handle, the non-dimensional bubble diameter is used to determine the boundary between the regions. From the Rayleigh solution [19], a rapid change of the bubble size occurs when the non-dimensional bubble diameter is between 0.4 and 0.6. Fig. 2 shows the time history of a collapsing bubble in a subcooled liquid. Here, it is assumed that the non-dimensional bubble diameter is 0.4 at a regions' boundary. The bubble collapse time of the Rayleigh solution [19] is a little shorter than that of Zwick and Plesset [20]. It is due to the fact that the latter considers the heat transfer effects.

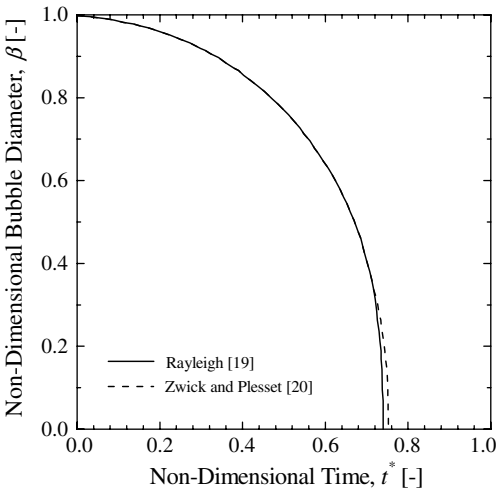

Fig. 2. Time history of the collapsing bubble in a subcooled liquid.

3.3. Bubble collapse time in the heat transfer-controlled region

The bubble collapse time is derived from the energy balance through a bubble interface. From the energy balance for the interface of a collapsing bubble, the following relationship is derived:

$$\dot{m}_c h_{fg} = h_c a_b (T_{sat} - T_f) \tag{7}$$

where $\dot{m}_c$, h_{fg}, and h_c are the mass transfer rate due to a condensation, the latent heat, and the condensation heat transfer coefficient, respectively.

The terms in the left- and right-hand sides in Eq. (7) are expressed as indicated by Eqs. (8) and (9), respectively.

$$\dot{m}_c h_{fg} = -\rho_g h_{fg} \frac{dv_b}{dt} = -\frac{\pi}{2} \rho_g h_{fg} D^2 \frac{dD}{dt} \tag{8}$$

and

$$h_c a_b (T_{sat} - T_f) = Nu_c \frac{k_f}{D} \cdot \pi D^2 \cdot (T_{sat} - T_f) \tag{9}$$

After matching Eqs. (8) and (9), the following equation is derived:

$$dt = -\frac{1}{2} \frac{\rho_g h_{fg} D}{Nu_c \cdot k_f (T_{sat} - T_f)} dD \tag{10}$$

An integration of Eq. (10) from the initial bubble diameter, or the bubble diameter at point D in Fig. 1, to the boundary bubble diameter D_b gives a bubble's residence time in the heat transfer-controlled region.

$$t_c = \frac{D_{sm}^2 - D_b^2}{4} \frac{\rho_g h_{fg}}{Nu_c \cdot k_f \Delta T_{sub}} \tag{11}$$

where t_c, D_{sm}, and ΔT_{sub} are the bubble residence time, the Sauter mean bubble diameter, and the liquid subcooling, respectively. In the present modeling approach the interfacial heat transfer coefficient or the Nusselt number plays a key role. The existing correlations for the interfacial heat transfer coefficient and Nusselt number are reviewed and evaluated based on the available experimental data in Appendix B.

4. Modeling of the condensation sink term

4.1. Derivation of the condensation sink term

As the two condensation-related sink terms of ϕ_{PC} and ϕ_{CO} are based on different physical phenomena, they should be modeled separately in an interfacial area transport equation. The term ϕ_{PC} is based on an interfacial heat transfer between bubbles and their surrounding liquid but the term ϕ_{CO} is based on a mechanical force balance through a bubble–liquid interface.

Once a bubble enters the inertia-controlled region, it is assumed to disappear through a total collapse. The fraction of bubbles with a smaller size than the boundary bubble size in the inertia-controlled region is defined as follows:

$$p_c = \text{probability}(D < D_b) \tag{12}$$

where p_c and D_b are the fraction of the bubbles in the inertia-controlled region and the bubble diameter at the region's boundary, respectively. If the boundary bubble diameter D_b and correspondingly the probability p_c can be calculated in this modeling approach, these two terms can be calculated separately. D is the bubble diameter and D_b may be chosen as the minimum bubble size in the thermal-controlled region. After these two terms are calculated separately, the ϕ_{CO} term of our model can be compared with Kocamusfaogullari and Ishii's model [9] for the bubble number density equation.

The probability can be calculated based on the bubble residence time of both regions. The time history of the collapsing bubble was calculated by Rayleigh [19] who used a hydrodynamic approach and arrived at the following expression for a non-dimensional time t^* as a function of the non-dimensional bubble diameter β, which is defined as D/D_0.

$$t^* = \frac{t}{D_0\sqrt{\frac{3\rho_f}{8P}}} = \int_\beta^1 \sqrt{\frac{\beta^3}{1-\beta^3}}\mathrm{d}\beta = f(\beta) \tag{13}$$

where D_0 is the initial bubble diameter which is assumed to be the Sauter mean bubble diameter, D_{sm}, and $f(\beta)$ can be calculated from the curve in Fig. 2. Zwick and Plesset [20] considered the effect of a heat transfer and suggested similar results to Rayleigh [19], as shown in Fig. 2. The residence times of the collapsing bubble both in the heat transfer-controlled region and the inertia-controlled region are calculated separately, if we can separate them by using the boundary bubble size.

The non-dimensional bubble diameter at the boundary is defined as $\beta_b = D_b/D_{sm}$. The residence times both in the heat transfer-controlled region and in the inertia-controlled region can be calculated by using Eq. (13).

$$\Delta t_{c,th} = D_0\sqrt{\frac{3\rho_f}{8P}}\int_{\beta_b}^1 \sqrt{\frac{\beta^3}{1-\beta^3}}\mathrm{d}\beta = D_0\sqrt{\frac{3\rho_f}{8P}}\cdot f(\beta_b) \tag{14}$$

$$\begin{aligned}\Delta t_{c,in} &= D_0\sqrt{\frac{3\rho_f}{8P}}\left(\int_0^1 \sqrt{\frac{\beta^3}{1-\beta^3}}\mathrm{d}\beta - \int_{\beta_b}^1 \sqrt{\frac{\beta^3}{1-\beta^3}}\mathrm{d}\beta\right)\\ &= D_0\sqrt{\frac{3\rho_f}{8P}}\cdot[f(0) - f(\beta_b)]\end{aligned} \tag{15}$$

where $\Delta t_{c,th}$ and $\Delta t_{c,in}$ are the residence times both in the heat transfer-controlled region and in the inertia-controlled region, respectively.

The probability that the bubble is in the inertia-controlled region can be calculated as follows:

$$p_c = \frac{\Delta t_{c,in}}{\Delta t_{c,th} + \Delta t_{c,in}} = \frac{f(0) - f(\beta_b)}{f(0)} \tag{16}$$

The condensation sink term of an IATE can be divided into two parts: one is related to a bubble collapse or disappearance, $\phi_{CO} = \pi D_b^2 R_{ph}$, when the bubble size is below the boundary bubble size, and the other is a volume contraction due to a condensation through a bubble interface, $\phi_{PC} = \frac{2}{3}\left(\frac{a_i}{\alpha}\right)\frac{\Gamma_g}{\rho_g}$, as shown in Eq. (5). The former term accounts for a variation of an IAC by a number density change due to an entire bubble collapse and the latter term represents a variation of an IAC with a constant bubble number density and a changing bubble size. When a bubble collapses, only the interfacial area changes until the bubble diameter reaches a boundary bubble diameter. During this initial stage the bubble number density is not changed. After the bubble diameter is below the boundary bubble diameter, the bubble number density is changed.

The IAC sink term due to a condensation in the heat transfer-controlled region can be calculated as follows:

$$\phi_{PC} = (1-p_c)\cdot n_b \cdot \frac{\mathrm{d}A_b}{\mathrm{d}t} = (1-p_c)\cdot n_b \cdot 2\pi D_{sm}\frac{\mathrm{d}D_{sm}}{\mathrm{d}t} \tag{17}$$

where n_b and A_i are the bubble number density and the interfacial area, respectively.

As the bubble number density and a change of the bubble diameter are expressed by

$$n_b = \psi \cdot \frac{a_i^3}{\alpha^2} \tag{18}$$

and

$$D_{sm}\cdot\frac{\mathrm{d}D_{sm}}{\mathrm{d}t} = -Nu_c\cdot\frac{2\cdot k_f\cdot(T_{sat}-T_f)}{\rho_g h_{fg}}, \tag{19}$$

then the condensation sink term in the heat transfer-controlled region can be expressed as follows:

$$\begin{aligned}\phi_{PC} &= -4\pi\cdot(1-p_c)\cdot n_b\cdot Nu_c\cdot\frac{k_f\cdot(T_{sat}-T_f)}{\rho_g h_{fg}}\\ &= -4\pi\cdot(1-p_c)\cdot\psi\cdot\frac{a_i^3}{\alpha^2}\cdot Nu_c\cdot Ja\cdot\alpha_t.\end{aligned} \tag{20}$$

where α_t is the thermal diffusivity and the Jakob number is expressed as follows:

$$Ja = \frac{\rho_f\cdot c_{p,f}\cdot(T_{sat}-T_f)}{\rho_g h_{fg}} \tag{21}$$

where $c_{p,f}$ is the specific heat of the liquid.

As the residence time of the inertia-controlled region calculated by Eq. (15) is very small when compared with that of the heat transfer-controlled region calculated by Eq. (11), the residence time in the heat transfer-controlled region is considered to be the total residence time. As a result the IAC sink term due to a condensation in the inertia-controlled region can be calculated as follows:

$$\phi_{CO} = R_{ph}\cdot\pi D_b^2 = -\pi D_b^2\cdot\psi\cdot\frac{a_i^3}{\alpha^2}\cdot\frac{1}{t_c} \tag{22}$$

The total IAC sink term due to a condensation is a sum of the condensation sink terms in both regions, as expressed in Eqs. (20) and (22), and it can be expressed as follows:

$$\phi_{CD} = -\pi\cdot n_b\cdot[4(1-p_c)\cdot Nu_c\cdot Ja\cdot\alpha_t + 1/t_c\cdot D_b^2] \tag{23}$$

4.2. Simulation results and discussion

There is a lot of data on the boiling phenomena but there is very little data on the condensation phenomena in a non-heated section. Zeitoun's experimental data [13] is available to evaluate an IATE modeling approach for a condensation. The test section is a vertical concentric annular test section. The inner tube, which has an outer diameter of 12.7 mm, consists of three axial sections. The middle section of the inner tube is a 30.6 cm long, thin-walled stainless-steel tube (0.25 mm thickness) that is electrically heated. This heated section is preceded and followed by two thick-walled copper tubes, 34 and 50 cm long, respectively. The outer tube is a 25.4 mm inner diameter plexiglass tube that permits a visual observation. There are eight sets of experimental data for the condensation phenomena in an unheated section but only three cases are available for an evaluation of a condensation modeling approach. Those three data sets provided void fraction and IAC data from the inlet to the outlet of the test section, while the other five data sets only provided very limited data points, which made it difficult to evaluate them. Table 1 shows the initial values used in the evaluation of the developed condensation sink term of an IATE. The condensation Nusselt number should be utilized to calculate the condensation sink term in the heat transfer-controlled region. In this simulation the following empirical correlation developed by Zeitoun [13] is used:

$$Nu_c = 2.04 \cdot Re_b^{0.61} \cdot \alpha^{0.328} \cdot Ja^{-0.308} \quad (24)$$

where Re_b, α, and Ja are the bubble Reynolds number, the void fraction, and the Jakob number, respectively.

Fig. 3 shows the calculated IAC changes and the separate contributions of a pressure change, a bubble breakup by a turbulence impact, a bubble coalescence by a random collision, and a condensation in the heat transfer-controlled region and in the inertia-controlled region for the case of Test Run C6 of Zeitoun [13]. For the case of Test Run C6 with an inlet pressure of 0.170 MPa, total mass flux of 492 kg/(m^2 s), and an inlet void fraction of 0.240, the contributions of a turbulence impact and a random collision are negligibly small when compared with the others. A bubble coalescence is considered to occur due to a random bubble collision induced by a turbulence in an ambient liquid and a bubble breakup is considered to occur due to a collision of a turbulent eddy with a bubble [4]. As these tests are performed for a low liquid velocity and a low void fraction, a random collision does not occur easily between the bubbles (bubble random collision) and between a bubble and a turbulent eddy (turbulent impact) due to the considerable distance between the bubbles. The contribution of a pressure change is as low as 2%. The main contribution is due to a condensation and the portion of the inertia-controlled region is about 16.8% for the case of Test Run C6. The overall agreement is reasonable between the simulated and measured data.

Table 1
The initial values used in the IATE simulation

Parameters\test cases	Run no. C6	Run no. C7	Run no. C8
Inlet pressure (MPa)	0.170	0.180	0.103
Inlet temperature (°C)	102.0	98.3	98.0
Total mass flux (kg/(m^2 s))	492.4	506.2	139.0
Inlet void fraction	0.240	0.204	0.163
Inlet IAC (1/m)	213.8	155.1	166.2

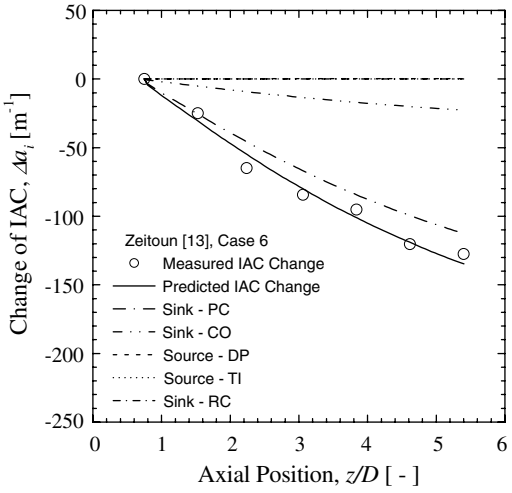

Fig. 3. Contributions of the simulated IAC source and sink terms and their comparison with the experimental data of Zeitoun [13]: Run no. C6.

Figs. 4 and 5 show the contributions of the simulated IAC source and sink terms and their comparison with the experimental data of Test Runs C7 and C8 of Zeitoun [13], respectively. The agreements between the prediction and the experimental data are also good for the case of Test Run C7 with an inlet pressure of 0.180 MPa, total mass flux of 506 kg/(m^2 s), and an inlet void fraction of 0.204, and Test Run C7 with an inlet pressure of 0.103 MPa, total

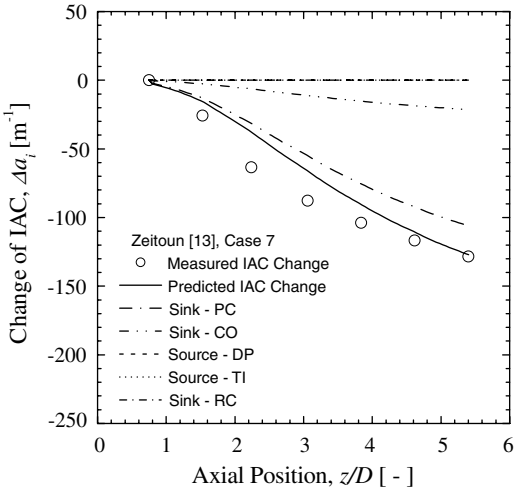

Fig. 4. Contributions of the simulated IAC source and sink terms and their comparison with the experimental data of Zeitoun [13]: Run no. C7.

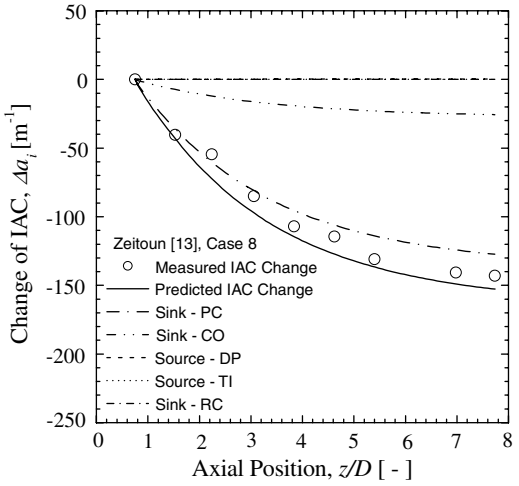

Fig. 5. Contributions of the simulated IAC source and sink terms and their comparison with the experimental data of Zeitoun [13]: Run no. C8.

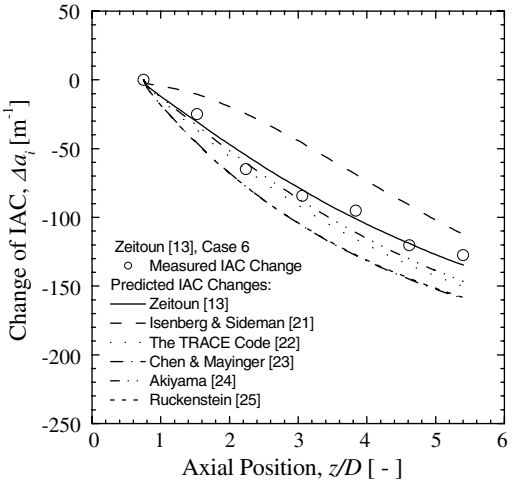

Fig. 7. Comparison of the simulated IAC changes for different Nusselt number correlations with the experimental data of Zeitoun [13]: Run no. C6.

mass flux of 139 kg/(m^2 s), and an inlet void fraction of 0.163, respectively.

Fig. 6 shows a comparison of the simulated IAC changes for different non-dimensional bubble diameters at the boundary with the experimental data of Zeitoun [13]. The IAC changes are simulated with different non-dimensional boundary bubble diameters of 0.1, 0.2, 0.3, 0.4, 0.5, and 0.6 for the experimental data of Test Run C6 of Zeitoun [13]. The simulation result shows that the agreement is the best with a non-dimensional bubble diameter of 0.4, which justifies the assumption of a threshold bubble diameter between the thermally-control region and the mechanically-control region.

Sensitivity analyses are also performed for different Nusselt number correlations. Figs. 7–9 show the comparisons of the simulated IAC changes for the different Nusselt number correlations with the experimental data of Test Runs C6, C7, and C8 of Zeitoun [13], respectively, and

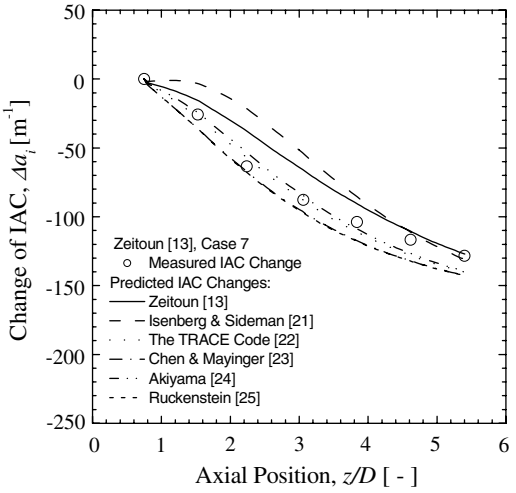

Fig. 8. Comparison of the simulated IAC changes for different Nusselt number correlations with the experimental data of Zeitoun [13]: Run no. C7.

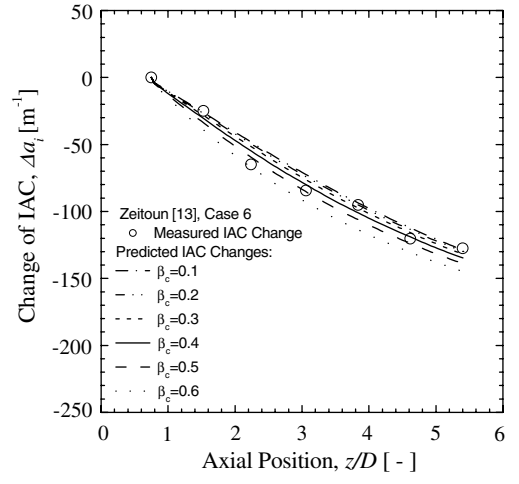

Fig. 6. Comparison of the simulated IAC changes for different non-dimensional bubble diameters at the boundary with the experimental data of Zeitoun [13].

Fig. 10 shows an overall comparison of the simulated IACs for different Nusselt number correlations with the experimental data of Zeitoun [13]. When Zeitoun [13]'s correlation is used to calculate the condensation Nusselt number, the present model can predict almost all of the data reasonably well except for the low IAC region where the condensation process is almost finished. The arithmetic mean of an absolute error of the predictions of the present model from the experimental IAC is 13.2%. The arithmetic mean of an absolute error ε is defined as follows:

$$\varepsilon = \frac{1}{n} \cdot \sum_{i=1}^{n} \left| \frac{a_{i,\mathrm{exp}} - a_{i,\mathrm{cor}}}{a_{i,\mathrm{exp}}} \right| \tag{25}$$

where n is the number of experimental data.

When Zeitoun [13]'s correlation for the condensation Nusselt number is replaced by Isenberg and Sideman

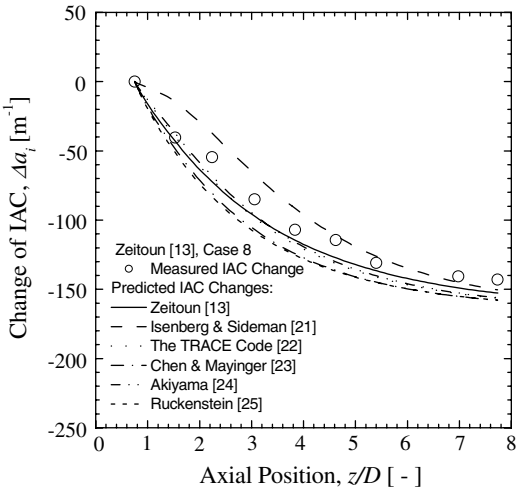

Fig. 9. Comparison of the simulated IAC changes for different Nusselt number correlations with the experimental data of Zeitoun [13]: Run no. C8.

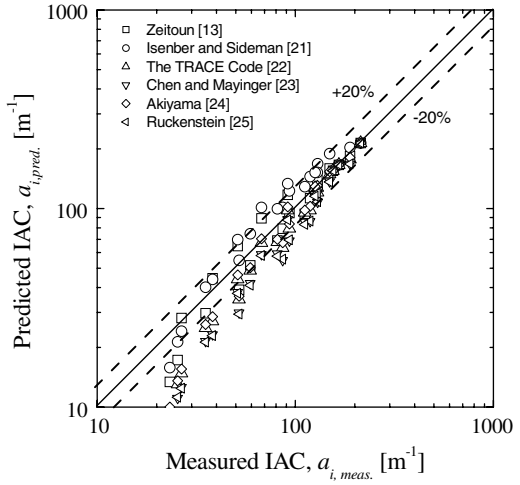

Fig. 10. Comparison of the simulated IACs for different Nusselt number correlations with the experimental data of Zeitoun [13].

[21]'s correlation, the correlation used in the TRACE code [22], and Chen and Mayinger [23]'s correlation, Akiyama [24]'s correlation, and Ruckenstein [25]'s correlation, the standard deviations of their predictions from the experimental IAC are 20.1%, 16.8%, 24.3%, 15.4%, and 24.8%, respectively. Chen and Mayinger [23]'s correlation, which is based on the data after a detachment, is used in the present comparison as the bulk condensation occurs after the bubble is detached from the wall. However, Warrier et al. [26]'s correlation could not be compared as it was expressed as a function of the Fourier number, which can not be estimated from Zeitoun's data. The simulation results show that the present model should be a promising modeling approach for the condensation phenomena of vapor bubbles in a subcooled liquid. The key correlation to solve this model is the correlation for the condensation Nusselt number.

When our model is to be applied to a high-pressure condition, the following discussion should be considered. Brucker and Sparrow [28] carried out experiments to investigate a direct contact condensation of saturated steam bubbles introduced into a quiescent subcooled water environment. Their experiments were performed in the range of pressures from 1.03 to 6.21 MPa, for a subcooling from 15 to 100 °C, and for initial bubble diameters of about 3 mm. Their experimental results showed that the bubble collapsing time increased with an increasing pressure and that the average heat transfer coefficients were in the order of 10^4 W/(m_2 °C) with modest variations with the pressure level, and the instantaneous heat transfer coefficients did not differ appreciably from the average heat transfer coefficients. However, as they did not provide any quantitative data to help us produce a condensation Nusselt number equation, we need to undertake more experiments to obtain a Nusselt number correlation applicable to a high-pressure condition to replace Eq. (24). As shown in Fig. 2, the non-dimensional bubble diameter is dependent on the non-dimensional time, which includes the pressure term to consider the pressure effect by itself. Therefore, the non-dimensional boundary bubble diameter of 0.4 could be applicable to a high-pressure condition as the collapsing mechanism of a bubble is theoretically similar to an atmospheric condition. However, from a comparison between tests with different pressure conditions, Brucker and Sparrow [28] found that a bubble interface was more compliant at higher pressures owing to a decrease of its surface tension and liquid viscosity with the temperature and was, therefore, more susceptible to oscillations. However, as they did not provide any quantitative data to help us select the value of a non-dimensional boundary bubble diameter, we need to undertake more experiments to identity the bubble collapsing mechanism at a high-pressure condition. Recently Lucas and Prasser [29] investigated the structure of a steam-water flow in a vertical pipe of 195.3 mm in inner diameter using their wire-mesh sensors under a high-pressure/high-temperature operation. This kind of data could be used to obtain a Nusselt number correlation and to obtain a value for a non-dimensional boundary bubble diameter at a high-pressure condition.

As another future work, the boiling phenomena can also be modeled with an existing or new modeling approach for a subcooled boiling in combination with this condensation modeling approach. Under some conditions of a subcooling and liquid velocity in a highly subcooled boiling, the coalesced bubbles on the heated surface were broken into many fine bubbles accompanied by a loud boiling noise which seemed to maintain a high heat flux at the beginning of the transition boiling, which is known as a micro-bubble emission boiling (MEB) [30]. It is considered that the boiling noise and the strong pressure fluctuation are generated by a rapid collapse of the large bubbles. Especially for a periodic type MEB a bubble growth and bubble generation occurred periodically. We have applied a simple model to model the bubble behavior on a condensation in a

two-phase flow system although the phenomena are extremely unsteady and complicated. It is expected that the present work will provide fundamental information to extend the modeling approach to a breakup of the plural coalescence bubbles grown on a large heated surface and the actual cases of the vibrations and pressure fluctuations generated in a two-phase flow system or a subcooled boiling.

5. Conclusions

As a step to develop a reliable IATE which can be applicable to a bubbly flow with a phase change, a model for the condensation sink term in an IATE is presented. Based on the bubble collapse phenomena, the condensation phenomena are considered to occur in two different regions: in the heat transfer-controlled region and in the inertia-controlled region. These two regions are identified by introducing the concept of a boundary bubble diameter, and then the bubble collapse time in the heat transfer-controlled region is calculated. Also the critical collapsing bubble size is calculated. The probability of an inertia-controlled region is calculated based on its residence time and a model for its condensation sink term is derived. The developed model is applied to a steady state one-group one-dimensional IATE, and evaluated against the existing experimental data sets which were obtained from a condensing steam-water flow through a non-heated annulus. The calculated results show that the present model can predict the experimental data reasonably well. The arithmetic mean of an absolute error of the predictions of the present model from the measured IAC is 13.2%. The contributions of a bubble breakup due to a turbulence impact, a bubble coalescence due to a random collision and a pressure change are found to be very small when compared with that of a condensation sink, as expected. Thus, the present model can be considered as a promising modeling approach for the condensation phenomena of vapor bubbles in a subcooled liquid. As a future work, the boiling phenomena can also be modeled with an existing or new modeling approach for a subcooled boiling in combination with this condensation modeling approach.

Acknowledgements

Two of the authors (Park and Lee) would like to express their appreciation to the Korea Research Foundation for their financial support on this subject.

Appendix A. Critical collapsing bubble diameter

As the bubble temperature decreases, it finally reaches a critical temperature after which a bubble can not maintain its shape any more. The critical collapsing bubble size is calculated in terms of the temperatures of the liquid and the bubble from the mechanical force balance through an interface. Fig. A.1 shows the saturated curve for the pressure and the temperature. When the subcooling of the liquid is low, the bubble is in the heat transfer-controlled region. However, as the subcooling becomes higher, the bubble moves into the inertia-controlled region. The duration of a bubble in the inertia-controlled region is very short and the bubble disappears, or moves into the bubble collapse region, when its diameter becomes smaller than the critical bubble size. From the mechanical force balance, the critical bubble size can be calculated.

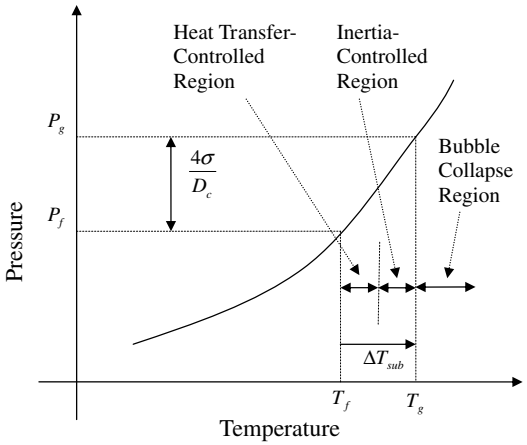

Fig. A.1. Saturated curve between the pressure and the temperature.

$$P_g - P_f = \frac{4\sigma}{D_c} \tag{A1}$$

where P_g, P_f, D_c, and σ are the pressure in the vapor bubble, the pressure in an ambient liquid, the critical collapsing bubble diameter, and the surface tension, respectively.

From the Clapeyron equation and the Clapeyron–Clausius approximation [27], the relationship between the pressure and the temperature is derived as follows:

$$\left.\frac{dP}{dT}\right)_{sat} = \frac{h_{fg}}{T(v_g - v_f)} \approx \frac{h_{fg}}{Tv_g} = \frac{h_{fg}}{RT^2}P \tag{A2}$$

where R, v_g, and v_f are the gas constant and the specific volumes in the vapor bubble and in an ambient liquid, respectively. If Eq. (A2) is integrated from P_g to P_f and from T_g to T_f, the following equation is derived:

$$\ln\frac{P_g}{P_f} = -\frac{h_{fg}}{R}\cdot\left(\frac{1}{T_g} - \frac{1}{T_f}\right) = \frac{h_{fg}}{R}\cdot\frac{T_g - T_f}{T_g T_f} \tag{A3}$$

where $P_g = P_{sat}(T_g)$ and $P_f = P_{sat}(T_f)$. The critical bubble diameter can be calculated by using Eqs. (A1) and (A3) as follows:

$$D_c = \frac{4\sigma}{P_f}\cdot\left(e^{\frac{h_{fg}}{R}\frac{T_g - T_f}{T_g T_f}} - 1\right)^{-1} \tag{A4}$$

The critical collapsing bubble size becomes infinitely large as the gas bubble temperature approaches the liquid temperature, as shown in Eq. (A4). In reality, D_c is very small when compared with the Sauter mean bubble diameter in

the heat transfer-controlled region. For the experimental data of Zeitoun [13] which is shown in Table 1, the critical collapsing bubble diameters are calculated to be 3.86, 1.52, and 25.0 μm for the conditions of Test Runs C6, C7, and C8, respectively. Except for the condition when the liquid temperature is near the saturated temperature, the bubble size is negligibly small.

Appendix B. Interfacial heat transfer coefficient and Nusselt number

The bubble condensation phenomena have been analyzed based on the energy balance around a collapsing bubble. For a collapsing spherical bubble in an ambient subcooled liquid the interfacial heat transfer coefficient can be expressed as follows by using a simple energy balance:

$$h_c = \frac{\rho_g h_{fg} \cdot (-dv_b/dt)}{A_b \cdot (T_{sat} - T_f)} = \frac{\rho_g h_{fg} \cdot (-dD_{sm}/dt)}{2 \cdot (T_{sat} - T_f)} \quad \text{(B1)}$$

where h_c, ρ_g, h_{fg}, A_b, v_b, and D_{sm} are the condensation heat transfer coefficient, vapor density, latent heat, interfacial area of a bubble, volume of a bubble, and Sauter mean bubble diameter, respectively.

The bubble condensation Nusselt number can also be expressed by using the local mean Sauter mean bubble diameter as follows:

$$Nu_c = \frac{h_c \cdot D_{sm}}{k_f} = -\frac{\rho_g h_{fg}}{2 \cdot k_f \cdot (T_{sat} - T_f)} \cdot D_{sm} \cdot \frac{dD_{sm}}{dt} \quad \text{(B2)}$$

where Nu_c and k_f are the condensation Nusselt number and liquid thermal conductivity, respectively.

Tables B.1 and B.2 show the available correlations for the non-dimensional bubble diameter and the condensation Nusselt number, respectively. The approaches to develop the correlations for the non-dimensional bubble diameter and the condensation Nusselt number are a little different from each other. Zeitoun [13] acquired experimental data for an interfacial heat transfer between bubbles and the surrounding subcooled water for a steam-water bubbly flow and developed a correlation for the condensation Nusselt number. For the case of Warrier et al. [26], a correlation for the non-dimensional bubble diameter is developed based on the measured bubble diameter and the presupposed condensation Nusselt number, and then the correlation for the condensation Nusselt number is developed based on the correlation for the non-dimensional bubble diameter. The non-dimensional bubble diameter is calculated based on the developed condensation Nusselt number. For the case of Chen and Mayinger [23], both the non-dimensional bubble diameter and the condensation Nusselt number are measured and correlated.

The existing correlations are evaluated based on the experimental data of Warrier et al. [26]. The flow channel is 1.83 m long, of which the heated section length is 0.30 m. A 0.61 m long flow development section is provided upstream of the heated section, while a 0.30 m long section is provided downstream of the heated section. In addition, transition sections, each 0.30 m long, are provided upstream and downstream of the test section. The flow channel is almost square in cross-section with a flow area of 16.33 cm^2. Warrier et al. [26] performed low

Table B.1
Bubble condensation models for the non-dimensional bubble diameter

Author	Non-dimensional bubble diameter	Prediction error (%)
Zeitoun [13]	$\beta = (1 - 5.67 \cdot Re_{b,0}^{0.61} \cdot \alpha^{0.328} \cdot Ja^{0.692} Fo_0)^{0.72}$	–
Isenberg and Sideman [21]	$\beta = (1 - 3/\sqrt{\pi} \cdot Ja \cdot Re_{b,0}^{1/2} \cdot Pr^{1/3} \cdot Fo_0)^{2/3}$	18.2
Chen and Mayinger [23]	$\beta = (1 - 0.56 \cdot Re_{b,0}^{0.7} \cdot Pr^{0.5} \cdot JaFo_0)^{0.9}$	33.1
Akiyama [24]	$\beta = (1 - 2.8 \cdot 0.37 \cdot Ja \cdot Re_{b,0}^{0.6} \cdot Pr^{1/3} \cdot Fo_0)^{1/1.4}$	18.8
Warrier et al. [26]	$\beta^{3/2} = 1 - 1.8 Re_{b,0}^{1/2} Pr^{1/3} Ja \cdot Fo \cdot [1 - 0.72 Ja^{9/10} Fo_0^{2/3}]$	7.9

Table B.2
Bubble condensation models for the condensation Nusselt number

Author	Condensation Nusselt number	Applicable range	Prediction error (%)
Zeitoun [13]	$Nu_c = 2.04 \cdot Re_b^{0.61} \cdot \alpha^{0.328} \cdot Ja^{-0.308}$	$2266 \leqslant Re_b \leqslant 7953$	–
Isenberg and Sideman [21]	$Nu_c = 1/\sqrt{\pi} \cdot Re_b^{1/2} \cdot Pr^{1/3}$	Non-available	30.2
TRACE Code [22]	$Nu_c = 116.7 \cdot \sqrt{Pr}$	$Re_b \geqslant 10{,}000$	65.0
	$Nu_c = 0.185 \cdot Re_b^{0.7} \cdot \sqrt{Pr}$	$400 \leqslant Re_b \leqslant 10{,}000$	
	$Nu_c = 2 + \left(0.4\sqrt{Re_b} + 0.06 \cdot Re_b^{2/3}\right) \cdot Pr^{0.4}$	$Re_b \leqslant 400$	
Chen and Mayinger [23]	$Nu_c = 0.6 \cdot Re_b^{0.6} \cdot Pr^{0.5}$ (before detachment)	$Re_b \leqslant 10{,}000$	96.1
	$Nu_c = 0.185 \cdot Re_b^{0.7} \cdot Pr^{0.5}$ (after detachment)		12.9
Akiyama [24]	$Nu_c = 0.37 \cdot Re_b^{0.6} \cdot Pr^{1/3}$	Non-available	28.0
Ruckenstein [25]	$Nu_c = \sqrt{4/\pi} \cdot (Re_b \cdot Pr)^{1/2}$	Non-available	172.5
Warrier et al. [26]	$Nu_c = 0.6 Re_b^{1/2} Pr^{1/3} \cdot [1 - 1.20 Ja^{9/10} Fo_0^{2/3}]$	$20 \leqslant Re_b \leqslant 700$	8.5

pressure subcooled flow boiling experiments by using a vertical flat plate heater to investigate the bubble collapse process and correlated the condensation Nusselt number by using the experimental data. The bubble Reynolds number ranges from 20 to 700.

Fig. B.1 shows the prediction of the experimental data for a non-dimensional bubble diameter from the existing correlations. The prediction of Chen and Mayinger's correlation [23] is the lowest when compared with the experimental data and also, the predictions of Akiyama's correlation [24] and Isenberg and Sideman's correlation [21] are a little lower than the experimental data. It is interesting that there is no available measurement data below 0.3 due to a rapid decrease of the bubble size in the later stage of a bubble collapse. The standard deviations of the predictions of the existing correlations from the experimental non-dimensional bubble diameter are listed in Table B.1.

Fig. B.2 shows the calculated bubble condensation Nusselt number versus the bubble Reynolds number based on the experimental data of Warrier et al. [26]. Ruckenstein's correlation [25] predicts about 2 times higher than the experimental data at a maximum and the correlations of Akiyama [24] and Isenberg and Sideman [21] predict the experimental data similarly. Chen and Mayinger's correlation – before a detachment [23] predicts higher values than the experimental data, while Chen and Mayinger's correlation – after a detachment [23] predicts similar values. It is because Warrier's data is also acquired for a detached or floating bubble in an ambient liquid. The correlation used in the TRACE code [22] predicts a little higher values than the experimental data. The standard deviations of the predictions of the existing correlations from the experimental condensation Nusselt number are listed in Table B.2.

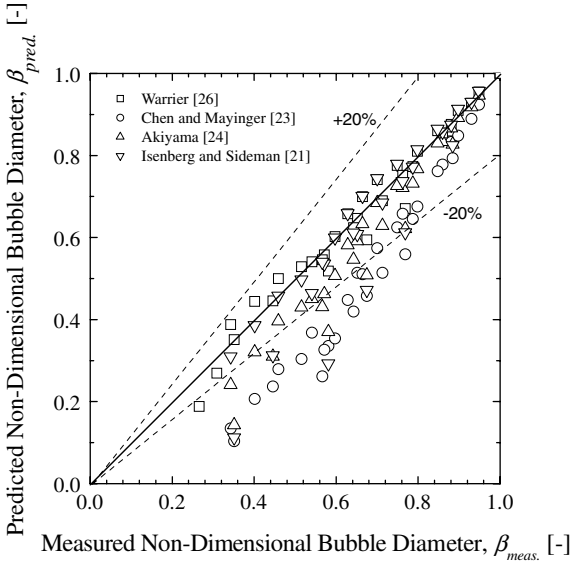

Fig. B.1. Predictions of Warrier et al. [26]'s experimental data for a non-dimensional bubble diameter from selected correlations.

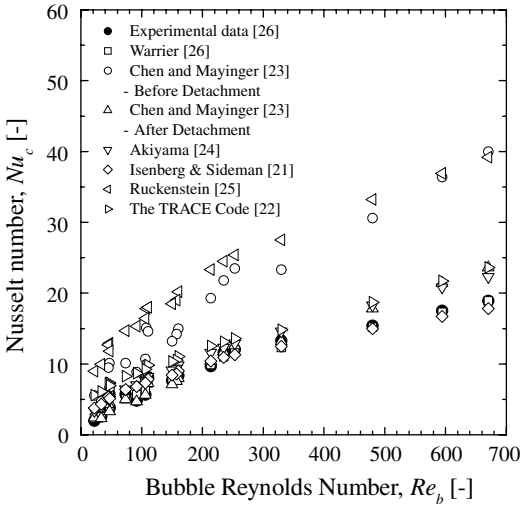

Fig. B.2. Predictions of Warrier et al. [26]'s experimental data for a condensation Nusselt number from selected correlations.

References

[1] G. Kocamustafaogullari, M. Ishii, Foundation of the interfacial area transport equation and its closure relations, Int. J. Heat Mass Transfer 38 (3) (1995) 481–493.
[2] M. Ishii, T. Hibiki, Thermo-Fluid Dynamic Theory of Two-Phase Flow, Elsevier Science, 2005.
[3] Q. Wu, S. Kim, M. Ishii, One-group interfacial area transport in vertical bubbly flow, Int. J. Heat Mass Transfer 41 (1998) 1103–1112.
[4] T. Hibiki, M. Ishii, One-group interfacial area transport of bubbly flows in vertical round tubes, Int. J. Heat Mass Transfer 43 (2000) 2711–2726.
[5] T. Hibiki, Y. Mi, R. Situ, M. Ishii, Interfacial area transport of vertical upward bubbly two-phase flow in an annulus, Int. J. Heat Mass Transfer 46 (2003) 4949–4962.
[6] T. Hibiki, M. Ishii, Two-group interfacial area transport equations at bubbly-to-slug flow transition, Nucl. Eng. Des. 202 (2000) 39–76.
[7] X. Sun, S. Kim, M. Ishii, S.G. Beus, Modeling of bubble coalescence and disintegration in confined upward two-phase flow, Nucl. Eng. Des. 230 (2004) 3–26.
[8] M. Ishii, S. Kim, J. Kelly, Development of interfacial area transport equation, Nucl. Eng. Technol. 37 (6) (2005) 525–536.
[9] G. Kocamustafaogullari, M. Ishii, Interfacial area and nucleation site density in boiling systems, Int. J. Heat Mass Transfer 26 (9) (1983) 1377–1387.
[10] T. Hibiki, M. Ishii, Active nucleation site density in boiling systems, Int. J. Heat Mass Transfer 46 (2003) 2587–2601.
[11] R. Situ, T. Hibiki, M. Ishii, M. Mori, Bubble lift-off size in forced convective subcooled boiling flow, Int. J. Heat Mass Transfer 48 (2005) 5536–5548.
[12] L.W. Florschuetz, B.T. Chao, On the mechanics of vapor bubble collapse, J. Heat Transfer (May) (1965) 209–220.
[13] O.M. Zeitoun, Subcooled flow boiling and condensation, Ph.D. Thesis, McMaster University, Canada, 1994.
[14] T. Hibiki, R. Situ, Y. Mi, M. Ishii, Modeling of bubble-layer thickness for formulation of one-dimensional interfacial area transport equation in subcooled boiling two-phase flow, Int. J. Heat Mass Transfer 46 (2003) 1409–1423.
[15] S. Kim, X. Sun, M. Ishii, S.G. Beus, F. Lincoln, Interfacial area transport and evaluation of source and sink terms for confined air–water bubbly flow, Nucl. Eng. Des. 219 (2002) 61–75.
[16] N. Zuber, The dynamics of vapor bubbles in nonuniform temperature fields, Int. J. Heat Mass Transfer 2 (1961) 83–98.

[17] A.H. Abdelmessih, F.C. Hooper, S. Nangia, Flow effects on bubble growth and collapse in surface boiling, Int. J. Heat Mass Transfer 15 (1972) 115–125.
[18] M.S. Plesset, On the stability of fluid flows with spherical symmetry, J. Appl. Phys. 25 (1) (1954) 96–98.
[19] J.W.S. Rayleigh, On the pressure developed in a liquid during the collapse of a spherical cavity, Philos. Mag. 34 (1917) 94–98.
[20] S.A. Zwick, M.S. Plesset, On the dynamics of small vapor bubbles in liquids, J. Math. Phys. 33 (1955) 308–330.
[21] J. Isenberg, S. Sideman, Direct contact heat transfer with change of phase: bubble condensation in immiscible liquids, Int. J. Heat Mass Transfer 13 (1970) 997–1011.
[22] J.W. Spore, J.S. Elson, S.J. Jolly-Woodruff, T.D. Knight, J.C. Lin, R.A. Nelson, K.O. Pasamehmetoglu, R.G. Steinke, C. Unal, TRAC-M/FORTRAN 90 (Version 3.0) – Theory Manual. LA-UR-00-910. Los Alamos National Laboratory, Los Alamos, New Mexico, USA, 2000.
[23] Y.M. Chen, F. Mayinger, Measurement of heat transfer at phase interface of condensing bubble, Int. J. Multiphase Flow 18 (1992) 877–890.
[24] M. Akiyama, Bubble collapse in subcooled boiling, Bull. JSME 16 (1973) 570–574.
[25] E. Ruckenstein, On heat transfer between vapor bubbles in motion and the boiling liquid from which they are generated, Chem. Eng. Sci. 10 (1959) 22–30.
[26] G.R. Warrier, N. Basu, V.K. Dhir, Interfacial heat transfer during subcooled flow boiling, Int. J. Heat Mass Transfer 45 (2002) 3947–3959.
[27] H.B. Callen, Thermodynamics and an Introduction to Thermostatistics, second ed., John Wiley & Sons, 1985, pp. 228-231.
[28] G.G. Brucker, E.M. Sparrow, Direct contact condensation of steam bubbles in water at high pressure, Int. J. Heat Mass Transfer 20 (1977) 371–381.
[29] D. Lucas, H.M. Prasser, Steam bubble condensation in sub-cooled water in case of co-current vertical pipe flow, Nucl. Eng. Des. 237 (2007) 497–508.
[30] K. Suzuki, T. Kokobu, M. Nakano, H. Kawamura, I. Ueno, H. Shida, O. Ogawa, Enhancement of heat transfer in subcooled boiling with microbubble emission, Exp. Thermal Fluid Sci. 29 (2005) 827–832.